Investigation of Passive Layers of Incoloy MA 956 and DIN 1.4575 for odontological applications

Maysa Terada, Rogério A. Marques, Angelo Fernando Padilha, Isolda Costa

Laboratório Nacional de Nanotecnologia, Av. Giuseppe Maximo Scolfaro, 10.000, Polo II de alta Tecnologia, CEP 13083-970, Campinas-SP- Brazil, maysa.terada@lnnano.org.br
Instituto de Pesquisas Energéticas e Nucleares, Centro Tecnológico de Ciência dos Materiais (CCTM), Av. Lineu Prestes, 2242, CEP 05508-900, São Paulo – SP - Brazil.
Escola Politécnica da Universidade de São Paulo, Departamento de Engenharia Metalúrgica e de Materiais, Av. Prof. Mello de Morais, 2463, CEP 05508-030, São Paulo - SP - Brazil.

Introduction

Metallic materials are widely used in orthodontic appliances as bands, arch wires, ligature wires, hooks, tubes, brackets and springs [1]. The use of ferromagnetic alloys is restricted due to the size of the implant [2,3], as it can move or heat during MRI analysis [4]. Most of MRI equipments generate magnetic fields of 1.5 T and some achieves 3.0 T, equivalent to 50,000 times the magnetic field of the Earth [3]. It was proven that small devices, as dental implants and dental prosthesis attachments, are not affected by MRI tests [5,6].

Both stainless steels investigated in this study, Incoloy MA 956 and DIN 1.4575, are ferromagnetic. MA 956 is produced by mechanical alloying followed by hot extrusion. Previous researches concluded that the Incoloy MA 956 has outstanding properties for applications as biomaterial [8-10] as the yttrium oxide improves the superalloy corrosion resistance [11]. In addition, the aluminum oxide layer formed at the outer porous layer favors osseointegration.

Experimental

The MA 956 investigated in the present study was produced by mechanical alloying and their chemical composition is shown in Table 1.

Table 1. Chemical composition (wt. %) of Incoloy MA 956 and DIN 1.4575.

	C	Cr	Ni	Mo	Si	Mn	others	Fe
DIN 1.4575	0.01	28.12	3.91	2.44	0.35	0.22	Nb=0.31	Bal.
Incoloy MA 956	0.02	21.26	0.09	0.16	0.07	0.14	Al=4.61 Y=0.42 Ti=0.39	Bal.

Samples of 0.90 cm² of Incoloy MA 956 were cut from a transversal section of extruded cylindrical bars (d = 30 mm) and then solution annealed at 1050 ºC for 1 h. Samples of 1 cm^2 of DIN 1.4575 were cut from a rolled sheet and then solution annealed at 1050 °C for 30 minutes.

All the samples were ground with silicon carbide paper up to #4,000, then rinsed with deionised water and immersed in PBS solution at 25 °C, whose composition is shown in Table 2. Initially few tests were carried out at 37 °C and others at 25 °C, but after comparing the results and the observation that there was no significant effect of the increase in temperature from 25 °C to 37 °C for the two tested materials, the electrochemical tests were performed at 25 ºC. Samples were analyzed by electrochemical techniques as EIS and potentiodynamic polarization curves.

Table 2 - Chemical composition (g L^{-1}) of the phosphate buffer solution (PBS), pH = 7.0.

NaCl	Na_2PO_4	KH_2PO_4
8.77	1.42	2.72

The electrochemical tests were performed using a three-electrode cell set-up, with a platinum wire and a saturated calomel electrode (SCE) as counter and reference electrodes, respectively. Electrochemical impedance spectroscopy (EIS) measurements were accomplished using a Gamry model EIS 300® frequency response analyzer coupled to a Gamry PCI 4/300 potentiostat. All EIS measurements were obtained in the potentiostatic mode at the stabilized open circuit potential after 24 hours of immersion. The amplitude of the sinusoidal signal was 10 mV (rms) and the investigated frequency was from 100 kHz to 10 mHz, with an acquisition rate of 6 points per decade. After the EIS tests, potentiodynamic polarization measurements were obtained in the range from the open circuit potential (OCP) up to the current reached 10 mA/cm^2, at a scan rate of 1 mV s^{-1}. After polarization tests, the tested surface was analyzed by scanning electron microscopy (SEM) using a Philips XL30 microscope. The reproducibility of the results was investigated by carrying out five tests for each material studied and the results were found to be reproducible.

Results and Discussion

The EIS results of both tested alloys after 24 h immersion in PBS are shown in Figure 1. The impedance modulus values at 0.01 Hz were of the order of 105 $k\Omega.cm^2$ for both materials. The Bode phase angle diagram for both SS show a very large peak from 102 Hz to approximately 1 Hz, indicating the interaction of more than one time constant. These results were supported by those obtained from fitting procedure.

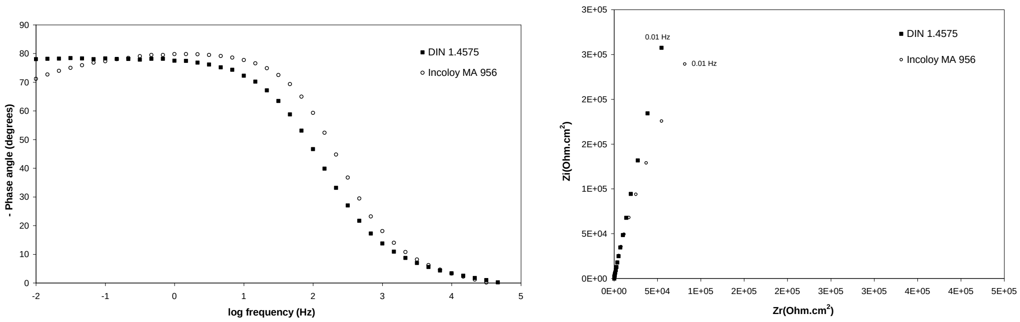

Figure 1: EIS diagrams obtained for MA 956, DIN 1.4575 and DIN 1.4460 high N solution annealed. EIS tests were carried out after 24 h of immersion in PBS solution at 25 ºC.

The potentiodynamic polarization curves obtained for both studied alloys shown in Figure 2 reveal that DIN 1.4575 presented breakdown potential around 1.1 V_{SCE} whereas the MA 956 showed large current increase at potentials of approximately 0.2 V_{SCE}. The current density increase at 1.1 V_{SCE} potential could be due to the oxygen evolution reaction instead of pitting. The samples were analyzed by scanning electron microscopy (SEM) after anodic polarization tests to investigate the presence or lack of pits.

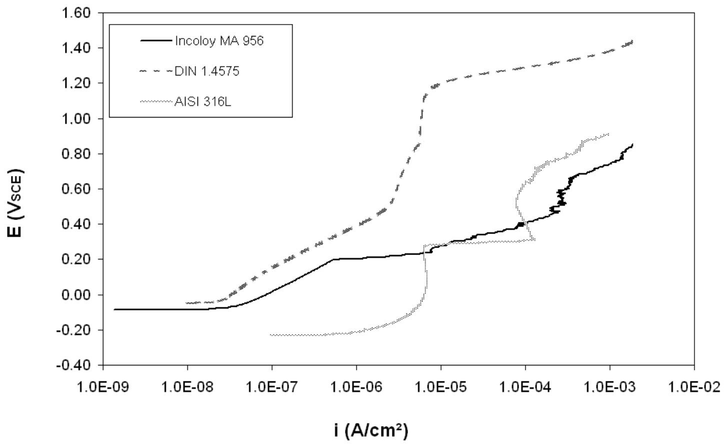

Figure 2: Potentiodynamic polarization curves for MA 956 and DIN 1.4575 SS solution annealed. Results obtained after 24 h of immersion in PBS solution at 25 ºC.

Conclusions

The electrochemical tests and surface observation after polarization tests showed that the passive film on the DIN 1.4575 SS is more resistant to corrosion than the Incoloy MA 956.
The electrochemical tests suggested that both stainless steels have a passive oxide film with a duplex nature, composed of an inner and more resistant layer, and an outer layer. The potentiodynamic polarization curves show higher corrosion rates associated to the Incoloy MA 956 comparatively to the DIN 1.4575, supporting the EIS results.

Acknowledgements

The authors acknowledge FAPESP and CAPES for the financial support.

References

[1] K.T. Oh, K.M. Kim, K.N. Kim, Properties of super stainless steel (UNS No. S32050) wire for orthodontic application, J. Dent. Res. 80 (2001) 1355
[2] P.F.J. New, B.R. Rosen, T.J. Brady, F.S. Buonanno, J.P. Kistler, C.T. Burt, W.S. Hinshaw, J.H. Newhouse, G.M. Pohost, J.M. Taveras. Potential hazards and artifacts of ferromagnetic and nanoferromagnetic surgical and dental materials and devices in Nuclear Resonance Imaging, Radiology 147 (1983) 139
[3] T.O. Woods, Stainless steels for medical and surgical applications. In: ASTM Symposium, USA, (2002) 82
[4] F.G. Shellock, J.S. Curtis, MR Imaging and biomedical implants, materials, and devices: an update review, Radiology 180 (1991) 541
[5] F.T. Iimuro, Magnetic Resonance Imaging artifacts and the magnetic attachment system, Dent. Mater. J. 13 (1994) 76
[6] C. Devge, A. Tjellström, H. Nellström, Magnetic Resonance Imaging in patients with dental implants: a clinical report, Int. J. Oral Maxillofac. Implants 12 (1997)
[7] M.L. Escudero, J.L. González-Carrasco, In vitro corrosion behavior of MA 956 superalloy, Biomaterials 15 (1994) 1175
[8] M.L. Escudero, J.L. González-Carrasco, M.C. García-Alonso, E. Ramirez, Eletrochemical impedance spectroscopy of preoxidized MA 956 superalloy during in vitro experiments, Biomaterials 16 (1995) 735
[9] M.L. Escudero, M.F. López, J. Ruiz, M.C. García-Alonso, H. Canahua, Comparative study of the corrosion behavior of MA-956 and conventional biomaterials, J. Biomed. Mater. Res. 31 (1996) 313
[10] P. Ginesan, G.D. Smith, Oxide scale formation on selected candidate combustor alloys in simulated gas turbine environments, J. Mater. Eng. 9 (1998) 337
[11] R.A. Antunes, Caracterização do comportamento frente à corrosão de um aço inoxidável austenítico para aplicações biomédicas com revestimentos PVD de TiN, TiCN e DLC. 2006. PhD Thesis – Instituto de Pesquisas Energéticas e Nucleares. São Paulo, 2006.